Journal of Coordination Chemistry

ISSN: 0095-8972 (Print) 1029-0389 (Online) Journal homepage: http://www.tandfonline.com/loi/gcoo20

Synthesis, characterization, equilibria and biological activity of dimethyltin(IV) complex with 1,4-piperazine

Mohamed R. Shehata, Mahmoud M.A. Mohamed, Mohamed M. Shoukry, Mohamed A. Hussein & Fatma M. Hussein

To cite this article: Mohamed R. Shehata, Mahmoud M.A. Mohamed, Mohamed M. Shoukry, Mohamed A. Hussein & Fatma M. Hussein (2015) Synthesis, characterization, equilibria and biological activity of dimethyltin(IV) complex with 1,4-piperazine, Journal of Coordination Chemistry, 68:6, 1101-1114, DOI: 10.1080/00958972.2015.1007962

To link to this article: http://dx.doi.org/10.1080/00958972.2015.1007962

Journal of Coordination Chemistry, 2015
Vol. 68, No. 6, 1101–1114, http://dx.doi.org/10.1080/00958972.2015.1007962

Synthesis, characterization, equilibria and biological activity of dimethyltin(IV) complex with 1,4-piperazine

MOHAMED R. SHEHATA†, MAHMOUD M.A. MOHAMED†, MOHAMED M. SHOUKRY*†‡, MOHAMED A. HUSSEIN§ and FATMA M. HUSSEIN†

†Faculty of Science, Department of Chemistry, University of Cairo, Cairo, A.R. Egypt
‡Faculty of Science, Department of Chemistry, Islamic University, Madinah, Kingdom of Saudi Arabia
§Faculty of Pharmacy, Department of Biochemistry, October 6th University, Cairo, A.R. Egypt

(*Received 28 December 2013; accepted 30 December 2014*)

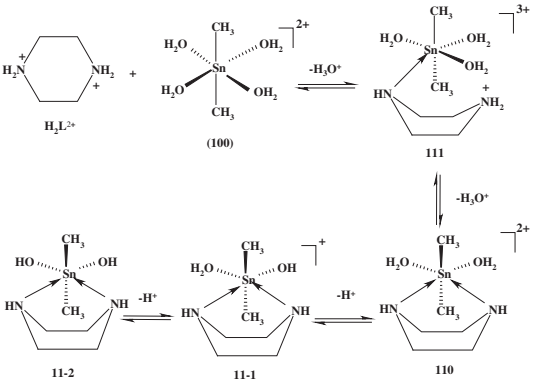

The interaction of dimethyltin(IV) dichloride (DMT) with 1,4-piperazine (PIP) was investigated. The complex formation equilibria of the complexes formed in solution were investigated. The stoichiometry and stability constants of the complexes formed in solution phase were determined at different temperatures and in solutions of dioxane–water mixtures of different dielectric constants. The equilibrium constant for the displacement of piperazine coordinated to dimethyltin(IV) by inosine as a representative of DNA was calculated. (DMT)(PIP)·$3H_2O$ was synthesized and characterized by elemental analysis, spectral, and thermal techniques. The antitumor activity of the complex was screened.

Keywords: Organotin(IV) complexes; 1,4-Piperazine; Equilibrium constants; Effect of temperature; Effect of solvent; Antitumor activity

1. Introduction

Metal complexes have been used for decades in medicine. For instance, cisplatin and the second generation complexes such as carboplatin and oxaliplatin are still the most widely

*Corresponding author. Email: shoukrymm@hotmail.com

used agents for the treatment of different types of cancer [1]. The success of cisplatin has aroused great interest in the study of metal complexes for possible applications in medicine [2–5].

The biological activity of organotin(IV) compounds has been well demonstrated. Organotin(IV) complexes with 1-methylpiperazine-dithiocarbamate were investigated by Sidek *et al.* [6, 7] and the complexes showed significant anti-microbial activity. Promising antitumor activity of organotin(IV) complexes was reported [8]. The *in vitro* antitumor activity of carboxylate-bridged dinuclear organotin(IV) complexes indicates better results than cis-platin [9]. Activity would be exerted by the diorganotin(IV) moieties [10] dissociated from the complexes. The latter would interact with nucleic acids, similarly as in the antitumor Pt(II) complexes. The antitumor activity is based on the ligand. It is generally accepted that coordination of organic ligands would facilitate transport across the cell membranes. If the complex is hydrolytically unstable, the R_2Sn moiety will be released too soon, and if it is too stable, it may be released slowly. Therefore, it is assumed that relatively long Sn–L bond was a requirement for the activity. Consequently, there is a relationship between the stability of the organotin compounds and their antitumor activity. With this in mind, and in conjunction with our previous studies on organotin(IV) complexes [11–15], the present paper aims to study the diorganotin(IV) complexes of 1,4-piperazine. 1,4-Piperazine is selected due to its hydrophobic nature which may help its organotin complex to enter into the cell.

2. Experimental

2.1. *Materials and reagents*

Dimethyltin(IV) dichloride (DMT) was provided by Merck Chem. Co. The ligand (PIP) was from Sigma Chem. Co. 1,4-Dioxane was provided by Aldrich Chem. Co. Sodium hydroxide stock solutions were prepared by diluting the content of BDH concentrated volumetric solution vials. These solutions were systematically checked by titration against potassium hydrogen phthalate. Human hepatocarcinoma cell line (Hep-G2), colon carcinoma cells (HCT-116), and lymphoblastic leukemia cells (1301) were purchased from ATCC, USA.

2.2. *Synthesis*

DMT(PIP)·$3H_2O$ was synthesized by mixing piperazine (0.086 g, 1 mM) and $(CH_3)_2SnCl_2$ (0.220 g, 1 mM) in 20 mL methanol. The mixture was stirred for 2 h. The resulting precipitate was filtered and washed thoroughly with diethyl ether (Yield 95%, MW = 359.9, m.p. 210–214 °C). Anal. Calcd for $C_6H_{16}SnN_2Cl_2·3H_2O$ (359.9): Calcd: C, 20.03; H, 6.16; N, 7.78; Cl, 19.70 %. Found: C, 19.9; H, 6.3; N, 7.7; Cl, 19.5%. IR (cm^{-1}): 3417 ν_{OH} (H_2O), 3000 ν_{NH} (piperazine), 560 $\nu_{Sn–C}$, 436, 455 $\nu_{Sn–N}$ and 421 $\nu_{Sn–O}$. ^1H NMR (δ, ppm): piperazine protons: 3.43 (broad) (NH) and 2.85 (–$N(CH_2CH_2)$N–). 0.85 $(CH_3)_2Sn$(IV).

2.3. *Procedure and measuring techniques*

The potentiometric titrations were performed using a Metrohm 686 titroprocessor equipped with a 665 dosimat (Switzerland-Herisaue). A Metrohm glass–calomel combined electrode and a thermometric probe were used. The titroprocessor and electrode were calibrated with standard buffer solutions, prepared according to NBS specifications [16]. The temperature

of the sample solutions was maintained at 25.0 ± 0.1 °C by circulating thermostatically controlled water through the jacket of a titration vessel. The ionic strength was adjusted to 0.1 M dm^{-3} with sodium nitrate. All potentiometric measurements were carried out under nitrogen. 1,4-Piperazine solution was prepared in the protonated form by dissolving in HNO_3 solution. The acid-dissociation constants of the protonated 1,4-piperazine were determined by titrating 0.05 mM. The hydroysis constants of dimethyltin(IV) were determined by titrating 0.05 mM. The formation constants of dimethyltin(IV)-piperazine complexes were determined by titrating solution mixture of dimethyltin(IV) (0.05 mM) and 1,4-piperazine (0.05 mM). The titrated solution mixtures each had a volume of 40 mL and the titrations were carried out at 0.1 dm^{-3} ionic strength (adjusted with $NaNO_3$). A standard 0.05 dm^{-3} NaOH solution was used as titrant. The pK_w values in dioxane–H_2O solutions were determined as described previously [17, 18]. For this purpose, various amounts of standard NaOH solution were added to a 0.10 M $NaNO_3$ solution. $[OH^-]$ was calculated from the amount of base added; $[H^+]$ was calculated from the pH value. The values obtained in this way for log $[OH^-][H^+]$ (log K_w) are −14.23, −14.50, −14.92, −15.12, and −15.63 for 25.0, 37.5, 50.0, 62.5, and 75.0% dioxane in H_2O, respectively.

The equilibrium constants were evaluated from titration data, defined by equations (1) and (2):

$$pM + qL + rH \rightleftharpoons MpLqHr \tag{1}$$

$$\beta_{pqr} = \frac{[M_pL_qH_r]}{[M]^p[L]^q[H]^r} \tag{2}$$

where M, L, and H represent dimethyltin(IV), 1,4-piperazine, and proton, respectively.

The stability constants were evaluated using the computer program MINIQUAD-75 [19]. The stoichiometry and stability constants of the complexes formed were determined by trying various possible composition models. The model selected was that which gave the best statistical fit and was chemically consistent with the magnitude of various residuals, as described elsewhere [19]. Tables 1–6 list the equilibrium constants together with their standard deviation derived from the MINIQUAD output. Concentration distribution diagrams were obtained using the program SPECIES [20].

The solid complexes were characterized by elemental analysis with analysis of carbon, hydrogen, and nitrogen carried out on a Perkin-Elmer 240C elemental analyzer. Infrared spectra were recorded on an 8001-PC FT-IR Shimadzu spectrophotometer using KBr pellets in the mid-infrared region 4000–400 cm^{-1}. ^1H NMR spectra were recorded on a Bruker AM300WB instrument at 298 K in DMSO-d_6. Chemical shifts are given in δppm downfield from TMS used as internal standard. Thermal analysis (TGA and DTA) were performed in nitrogen with a TGA-50 Shimadzu thermogravimetric analyzer and DTA-50 Shimadzu differential thermal analyzer. The potential characteristics are as follows: heating rate: 10 K min^{-1}, sample size: 10–15 mg for TAG, and 20 mg for DTA, temperature range: room temperature to 300 °C.

2.4. *Antitumor activity*

The piperazine complex was screened for its cytotoxicity against colon carcinoma (HCT 116), heptacellular carcinoma (HEP-G2), and T-lymphocyte (1301 cells) cancer cells using the protocol described previously [21, 22].

2.5. *Anti-inflammatory activity*

The anti-inflammatory activity studies were carried out following a reported method of Winter *et al.* [23]. Rats (180–200 g) were divided into five different groups each of six animals. At the beginning, the thickness of the left paw was measured. They were treated orally with the tested compounds, at 30 mg kg^{-1} body weight or indomethacin 600 mg kg^{-1} as a reference standard. After 30 min of administration, the inflammation was induced by S.C. injection of 0.1 mL of 6% formalin solution in normal saline. The right hind paw was injected with an equal volume of saline. The difference in thickness between the two paws gave the swelling induced by formalin. The anti-inflammatory efficacy was estimated by comparing the swelling of the treated with the control. The difference in thickness was recorded after 30, 60, 90, and 120 min.

3. Results and discussion

3.1. *Complex formation equilibria*

The acid-dissociation constants of protonated 1,4-piperazine were determined under the same experimental conditions of ionic strength, solvent composition, and temperature which are used for the study of organotin(IV) complex equilibria. The overall protonation constants ($\log \beta_{011}$ and $\log \beta_{012}$) were calculated. The values obtained are in good agreement with literature data [24] after considering changes in experimental condition.

The hydrolysis of dimethyltin(IV) cation in aqueous solution was studied by several research groups [25–29]. The potentimetric data were fitted considering the formation of the species 10-1, 10-2, 10-3, 10-4, 10-4, 20-3, and 20-4, where the numbers are stoichiometric coefficient of dimethyltin(IV), 1,4-piperazine and proton, respectively, as given in equation (1). The negative numbers mean loss of proton, i.e. formation of hydrolyzed dimethyltin(IV) species. The dimerization ability of aquo–hydroxo complexes is described by the general equilibrium:

$$2[(DMT)(H_2O)_3(OH]^+ \rightleftharpoons [(DMT)_2(HO)_2(H_2O)_4]^{2+} + 2H_2O^+ \tag{3}$$

The dimerization constant (K_d) can be obtained by equation (4):

$$\log K_d = \log \beta_{202} - 2 \log \beta_{10\text{-}1} \tag{4}$$

In the same way the dimerization constant of the species 20-4 is calculated by equation (5) [30]:

$$\log K_d = \log \beta_{20\text{-}4} - 2 \log \beta_{10\text{-}2} \tag{5}$$

The potentiometric titration curve of protonated piperazine in the presence and absence of dimethyltin(IV) are compared. The complex titration curve is significantly lower than the piperazine curve, figure 1. This corresponds to formation of a complex species through the release of hydrogen ion. The complex formation equilibria were investigated taking into

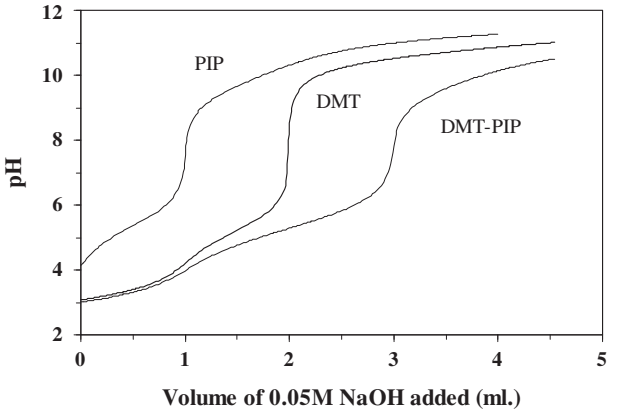

Figure 1. Potentiometric titration curve of PIP (0.05 mM) in the presence and absence of DMT.

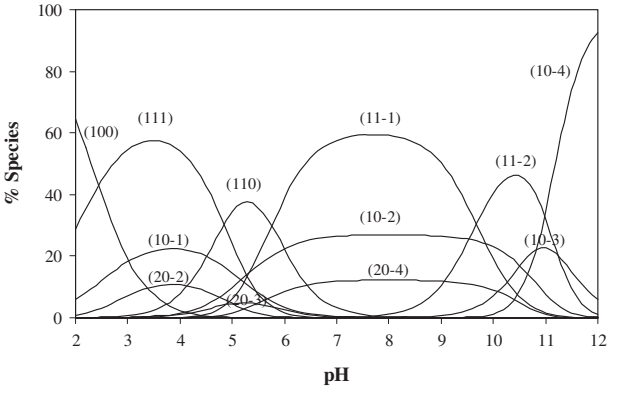

Figure 2. Concentration distribution of various species as a function of pH in the PIP–DMT system.

consideration the acid–base equilibria of 1,4-piperazine and hydrolysis of dimethyltin(IV) ion. The titration data at 25 °C were fitted with model composed of the 110, 111, 11-1, and 11-2 species, according to scheme 1.

The pK_a of coordinated waters are calculated by equations (6) and (7) [31]:

$$pK_{a1} = \log \beta_{110} - \log \beta_{11\text{-}1} \tag{6}$$

$$pk_{a2} = \log \beta_{11\text{-}1} - \log \beta_{11\text{-}2} \tag{7}$$

The calculated values of 5.57 (for the pK_{a1}) and 9.68 (for pk_{a2}) are higher than those of water molecules coordinated to free dimethyltin(IV) ion. This may be explained on the basis that coordination of 1,4-piperazine will decrease the electrophilicity of tin and hence the coordinated water will be weakly bound and consequently will be less acidic.

The concentration distribution diagram of DMT–PIP species provides a useful picture of the organotin binding with PIP as a function of pH, figure 2. The protonated complex, 111,

predominates at lower pH between pH 2.4 and 4.8 and reaches a maximum concentration of 57% at pH 3.4. The deprotonated complex 110 predominates between pH 4.8 and 5.8 with maximum concentration of 38% at pH 5.2. The hydrolyzed form 11-1 predominates between pH 5.8 and 9.8 with maximum formation percentage of 60% at pH 7.8. The main species in the physiological pH range are 110 and 11-1 species. Therefore, the interaction of DMT complex with DNA constituent, the main target in the chemotherapy, is quite feasible.

The thermodynamic parameters $\Delta H°$ and $\Delta S°$ were obtained by a linear least squares fit of $\ln K$ *vs.* $1/T$ ($\ln K = -\Delta H°/RT + \Delta S°/R$), leading to an intercept at $\Delta S°/R$ and a slope of $-\Delta H°/R$. The results obtained are summarized in table 7 and interpreted as follows: (a) The protonated reactions of 1,4-piperazine (1) and (2) indicated in table 7 are exothermic. Three factors affect protonated reactions: (i) the interaction of hydrogen ion with piperazine is exothermic, (ii) desolvation of piperazine which is an endothermic, and (iii) the configuration and the arrangement of the hydrogen bonds around the free and protonated piperazine. This may be explained as the premise that desolvation of piperazine is endothermic; this is confirmed by a positive $\Delta S°$ for the reaction. (b) Surprisingly, the complexation reaction (3) between DMT and piperazine is endothermic with $\Delta H°$ of 58.8 kJ M^{-1}. This is similar to what was found by Kramer-Schnabel [32] and can be interpreted as above by assuming that the enthalpy change is a net summation of two opposing effects, i.e. the exothermic complexation and the endothermic liberation of ordered water hydrogen. This is confirmed by large $\Delta S°$, 406 J^{-1} K^{-1} M^{-1}, giving negative $\Delta G°$ value, −62.4 kJ M^{-1}. The other complex formation reactions (4–6) are exothermic as usual.

Table 1. Protonation constants of 1,4-piperazine in water at different temperatures.

L H[a]	log β[b]		
	15 °C	20 °C	25 °C
1 1	9.98(0.01)	9.86(0.01)	9.75(0.04)
1 2	15.60(0.03)	15.35(0.02)	15.10(0.06)
	30 °C	35 °C	
1 1	9.60(0.03)	9.49(0.03)	
1 2	14.79(0.05)	14.55(0.03)	

[a]L and H are the stoichiometric coefficient corresponding to 1,4-piperazine and H^+, respectively.
[b]Standard deviations are given in parentheses; Sum of square of residuals are less than 4×10^{-7}.

Table 2. Protonation constants of 1,4-piperazine at 25 °C in dioxane–water mixture (V/V) solutions of different compositions.

L H[a]	log β[b]		
	12.5%	25%	37.5%
1 1	9.78(0.01)	9.66(0.01)	9.50(0.03)
1 2	15.24(0.03)	15.01(0.04)	15.01(0.07)
	50%	62.5%	75%
1 1	9.35(0.02)	9.25(0.03)	9.04(0.04)
1 2	14.31(0.06)	14.10(0.07)	13.81(0.09)

[a]L and H are the stoichiometric coefficient corresponding to 1,4-piperazine and H^+, respectively.
[b]Standard deviations are given in parentheses; Sum of square of residuals are less than 2×10^{-7}.

It is reported that the "effective" or "equivalent solution" dielectric constants in protein [33] or active site cavities of enzymes [34] are small compared to that in bulk water. Estimates for the dielectric constants in such locations range from 30 to 70 [35, 36]. Hence by using aqueous solutions containing dioxane, one may expect to simulate to some degree the situation in active site cavities [33], hence to extrapolate the data to physiological conditions. The results of the medium effect on the equilibrium constants given in tables 2, 4, and 6 are interpreted as: (a) The hydrolysis constants of DMT increase linearly with

Table 3. Acid-base equilibria of dimethyltin(IV) in water at different temperatures.

M L H[a]	log β[b]		
	15 °C	20 °C	25 °C
1 0 −1	−3.56(0.01)	−3.31(0.01)	−3.03(0.01)
1 0 −2	−9.05(0.01)	−8.64(0.01)	−8.21(0.01)
1 0 −3	−19.79(0.04)	−19.27(0.05)	−18.73(0.03)
1 0 −4	−30.41(0.04)	−39.71(0.02)	−29.54(0.02)
2 0 −2	−4.23(0.01)	−3.77(0.01)	−3.12(0.01)
2 0 −3	−9.52(0.01)	−8.91(0.02)	−8.13(0.02)
2 0 −4	−15.23(0.01)	−14.44(0.01)	−13.59(0.02)
	30 °C	35 °C	
1 0 −1	−2.81(0.01)	−2.49(0.02)	
1 0 −2	−7.91(0.02)	−7.54(0.02)	
1 0 −3	−18.38(0.05)	−17.95(0.06)	
1 0 −4	−28.71(0.02)	−28.20(0.03)	
2 0 −2	−2.87(0.02)	−2.27(0.03)	
2 0 −3	−7.84(0.04)	−7.11(0.04)	
2 0 −4	−13.06(0.04)	−12.34(0.04)	

[a]M, L and H are the stoichiometric coefficient corresponding to dimethyltin(IV), ligand and H^+, respectively.
[b]Standard deviations are given in parentheses; Sum of square of residuals are less than 5×10^{-7}.

Table 4. Acid-base equilibria of dimethyltin(IV) at 25 °C in dioxane–water mixture (V/V) solutions of different compositions.

M L H[a]	log β[b]		
	12.5%	25%	37.5%
1 0 −1	−3.27(0.01)	−3.39(0.00)	−3.53(0.01)
1 0 −2	−8.70(0.02)	−8.99(0.01)	−9.23(0.01)
1 0 −3	−19.53(0.06)	−19.83(0.01)	−20.18(0.02)
1 0 −4	−30.09(0.03)	−31.30(0.01)	−31.83(0.01)
2 0 −2	−3.68(0.02)	−3.92(0.01)	−4.17(0.01)
2 0 −3	−8.94(0.05)	−9.27(0.04)	−9.61(0.03)
2 0 −4	−14.52(0.04)	−15.11(0.03)	−15.59(0.03)
	50%	62.5%	75%
1 0 −1	−3.60(0.01)	−3.68(0.01)	−3.98(0.02)
1 0 −2	−9.43(0.01)	−9.62(0.02)	−9.93(0.05)
1 0 −3	−20.58(0.02)	−20.89(0.04)	−21.35(0.09)
1 0 −4	−32.52(0.02)	−33.26(0.05)	−33.74(0.08)
2 0 −2	−4.30(0.01)	−4.47(0.01)	−4.90(0.01)
2 0 −3	−9.78(0.04)	−9.90(0.03)	−10.10(0.01)
2 0 −4	−16.03(0.04)	−16.51(0.04)	−16.96(0.02)

[a]M, L and H are the stoichiometric coefficient corresponding to dimethyltin(IV), 1,4-piperazine and H^+, respectively.
[b]Standard deviations are given in parentheses; Sum of square of residuals are less than 10^{-7}.

Table 5. Formation constants of dimethyltin(IV)-1,4-piperazine complexes in water at different temperatures.

M L H[a]	log β[b]		
1 1 0	15 °C	20 °C	25 °C
1 1 1	10.61(0.01)	10.73(0.01)	10.95(0.02)
1 1–1	15.68(0.01)	15.75(0.01)	15.80(0.02)
1 1–2	4.71(0.01)	4.90(0.01)	5.20(0.05)
	−5.20(0.01)	−4.93(0.01)	−4.48(0.05)
	30 °C	35 °C	
1 1 0	11.12(0.04)	11.28(0.03)	
1 1 1	15.88(0.04)	15.96(0.03)	
1 1–1	5.44(0.03)	5.70(0.03)	
1 1–2	−4.10(0.02)	−3.69(0.02)	

[a]M, L and H are the stoichiometric coefficient corresponding to dimethyltin(IV), 1,4-piperazine and H^+, respectively.
[b]Standard deviations are given in parentheses; Sum of square of residuals are less than 5×10^{-7}.

Table 6. Formation constants of dimethyltin(IV)-1,4-piperazine complexes at 25 °C in dioxane–water mixture (V/V) solutions of different compositions.

M L H[a]	log β[b]		
	12.5%	25%	37.5%
1 1 0	11.53(0.09)	11.38(0.07)	11.25(0.07)
1 1 1	16.29(0.08)	16.15(0.08)	15.95(0.08)
1 1–1	5.85(0.08)	5.70(0.06)	5.62(0.07)
1 1–2	−3.76(0.07)	−3.80(0.07)	−3.81(0.08)
	50%	62.5%	75%
1 1 0	11.08(0.07)	10.76(0.09)	10.50(0.09)
1 1 1	15.65(0.07)	15.26(0.09)	14.78(0.01)
1 1–1	5.30(0.06)	5.10(0.08)	5.00(0.02)

[a]M, L and H are the stoichiometric coefficient corresponding to dimethyltin(IV), 1,4-piperazine and H^+, respectively.
[b]Standard deviations are given in parentheses; Sum of square of residuals are less than 5×10^{-7}.

increasing amount of dioxane in the medium. This may be correlated with the ability of solvent of relatively low dielectric constant to increase the electrostatic forces between proton and hydrolyzed form of DMT. (b) The protonation constants of piperazine and formation constants of DMT complexes with piperazine decreases with increasing dioxane content of the medium. This may be explained in terms of solvation of hydrophobic piperazine with the nonpolar dioxane. This will lead to decreases in the stability of piperazine-H^+ and piperazine-$(CH_3)Sn^{2+}$ complexes. These results are in accord with those found for $(CH_3)_2Sn^{2+}$-glycoxamine [37].

3.2. *Displacement reaction of 1,4-piperazine by DNA constituents*

It was shown above that N-donor ligands such as DNA constituents have affinity for $(CH_3)_2Sn$(IV), which may have important biological implications since the interaction with DNA is thought to be responsible for the antitumor activity of related complexes [38]. The antitumor activity of $(CH_3)_2Sn$-(amine) complex is based on the replacement of the amine by DNA. Consequently, the equilibrium constant for such conversion is of biological

significance. Considering inosine as a typical DNA constituent (represented by HA) and piperazine (represented by B), the equilibria involved in complex-formation and displacement reactions may be presented as:

$$HA \rightleftharpoons H^+ + A^-$$

$$\underset{(100)}{(CH_3)_2Sn^{2+}} + \underset{(110)}{A^-} \rightleftharpoons (CH_3)_2Sn\ (A)^+ \tag{8a}$$

$$\beta_{110}(CH_3)_2Sn\ (A)^+ = [(CH_3)_2Sn\ (A)^+]\ /[(CH_3)_2Sn^{2+}][A^-] \tag{8b}$$

$$\underset{(100)}{[(CH_3)_2Sn]^{2+}} + \underset{(110)}{B} \rightleftharpoons (CH_3)_2SnB^{2+} \tag{9a}$$

$$\beta_{110}(CH_3)_2SnB^{2+} = [(CH_3)_2SnB^{2+}]/[(CH_3)_2Sn^{2+}][B] \tag{9b}$$

$$(CH_3)_2Sn\ (B)^{2+} + A^- \overset{Keq}{\rightleftharpoons} (CH_3)_2Sn(A)^+ + B \tag{10a}$$

The equilibrium constant for the displacement reaction is given by:

$$K_{eq} = [(CH_3)_2Sn(A)^+][B]/[[([CH_3)_2Sn(B)^{2+}]][A^-] \tag{10b}$$

Substitution results in:

$$K_{eq} = \beta_{110}[(CH_3)_2Sn\ (A)]^+/\beta_{110}[(CH_3)_2Sn\ (B)]^{2+} \tag{11}$$

$$\log K_{eq} = \log \beta_{110}(CH_3)_2Sn\ (A)^+ - \log \beta_{110}(CH_3)_2Sn(B)^{2+} \tag{12}$$

The value of log β_{110} for $[(CH_3)_2SnB]^{2+}$ complex taken from table 5 amounts to 10.95 at 25 °C. The log β_{110} values for $(CH_3)_2Sn$-DNA constituents complexes [15] together with the equilibrium constants of displacement reaction calculated by equation (12) are given in table 8. These values clearly indicate the ability of DNA to displace 1,4-piperazine from its dimethyltin(IV) complex and to what extent the amine complex can interact with the DNA constituents, the main target in tumor chemotherapy. Comparison of the values of equilibrium constant of the displacement reaction for the different DNA constituents reveals that the nucleotides IMP and GMP have the highest values. This can be explained on the basis

Table 7. Thermodynamic parameters for the equilibria of DMT–PIP complexes.

Equilibrium[a]	$\Delta H°$ kJM^{-1}	$\Delta S°$ kJ^{-1} M^{-1}	$\Delta G°$ kJM^{-1}
PIP			
(1) $L + H^+ \rightleftharpoons LH^+$			
	−42.1(5)	45.0(5)	−55.5(7)
(2) $LH^+ + H^+ \rightleftharpoons LH_2^{2+}$			
	−48.2(6)	59.6(6)	−66.0(8)
DMT–PIP			
(3) $[M(H_2O)_4]^{2+} + L \rightleftharpoons M(H_2O)_2L^{2+} + 2H_2O$			
	58.8(5)	406(4)	−62.4(6)
(4) $M(H_2O)_2L^{2+} + H_3O^+ \rightleftharpoons M(H_2O)_3LH^{3+}$			
	−35.3(3)	−25.8(3)	−27.8(4)
(5) $M(H_2O)_2L^{2+} + OH^- \rightleftharpoons M(H_2O)(OH)L^+ + H_2O$			
	−26.8(3)	20.0(3)	−32.8(5)
(6) $M(H_2O)(OH)L^+ + OH^- \rightleftharpoons M(OH)_2L + H_2O$			
	−45.1(4)	33.7(4)	−55.2(6)

[a]M and L denote $(Me)_2Sn$ and piperazine (Pip); standard deviations (in the last digit) are given in parentheses.

Table 8. Equilibrium constants for displacement of coordinated 1,4-piperazine by DNA constituents at 25 °C and 0.1 M $NaNO_3$.

DNA	$\log \beta_{110}$ DMT-DNA	$\log K_{eq}$
Inosine	8.13	−2.82
Inosine-5′-monophosphate	11.90	0.95
Guanosine-5′-monophosphate	12.34	2.61
Adenine	10.01	−0.94
Adenosine	4.41	−6.54
Adenosine-5′-monophosphate	6.07	−4.88
Uracil	9.34	−1.61
Thymine	9.61	−1.34
Thymidine	9.25	−1.7
Cytosine	4.44	−6.51
Cytidine	3.77	−7.18

of the different columbic force of attraction between the dipositively charged diorganotin (IV) ion and IMP or GMP having extra negative charges on the phosphate group. The increase of columbic force of attraction between diorganotin(IV) and IMP or GMP and the role of phosphate of the DNA sugar backbone in acting as an anchoring site for tin [10] will facilitate the release of coordinated 1,4-piperazine.

3.3. *Solid complex characterization*

Characteristic IR absorption bands of the complex and corresponding free ligand (piperazine) from 4000 to 400 cm^{-1} are compared. The band at 3417 in the spectrum of DMT–PIP complex corresponds to ν(OH) of water. A sharp band at 3208 cm^{-1} ν(NH) in the infrared spectrum of free piperazine is broadened and shifted to 3000 cm^{-1} in the spectrum of DMT–PIP complex. The bands at 2989, 2951, and 2857 cm^{-1} corresponding to ν(CH) in free PIP are shifted to 2916 and 2831 cm^{-1} in DMT–PIP complex. The bending vibrations, δ(NH) at 1623, 1566, and 1558 cm^{-1} in free piperazine are shifted to 1632 and 1581 cm^{-1}

in DMT–PIP complex. The absorption at 565 cm^{-1} of ν(Sn–C) in free DMT is shifted to 560 cm^{-1} in DMT–PIP complex. The ν(Sn–C) for diorganotin(IV) complexes of monomethyl glutarate was reported to occur at 525–555 cm^{-1} [39]. The vibrations at 436 and 455 cm^{-1} in DMT–PIP correspond to ν(Sn–N) (imine) stretching vibration [40]. The vibration at 421 cm^{-1} in DMT–PIP complex is ν(Sn–O) of coordinated water in the complex [41]. Therefore, the complex is formed by coordination of piperazine N atoms to tin(IV), with the presence of coordinated water.

The ^{1}H NMR spectra of piperazine and its organotin(IV) complex were recorded in DMSO-d_6 because this is the only solvent which dissolves the ligand and complex. The ^{1}H NMR resonances were assigned on the basis of chemical shifts. ^{1}H NMR spectrum of uncomplexed 1,4-piperazine shows NH and –N(CH_2–CH_2)N– resonances at δ = 3.0 (broad) and 2.67 ppm, respectively. These signals were downfield shifted to 3.4 (broad) and 2.85 ppm, respectively, upon complex formation. The $(CH_3)_2$Sn(IV) proton signal occurs at 1.04 ppm.

The TGA for the complexes were carried out from room temperature to 200 °C. The dimethyltin(IV) complex of piperazine gives a decomposition stage corresponding to loss of three water molecules. The expected and observed mass losses are 15.00 and 14.827%, respectively.

Based on analytical data, spectral, and thermal analysis of dimethyltin(IV)-1,4-piperazine complex, the complex is assumed to have the following structure.

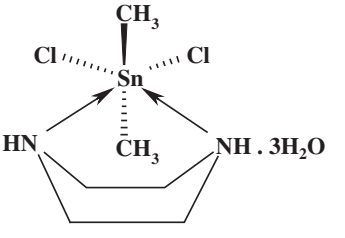

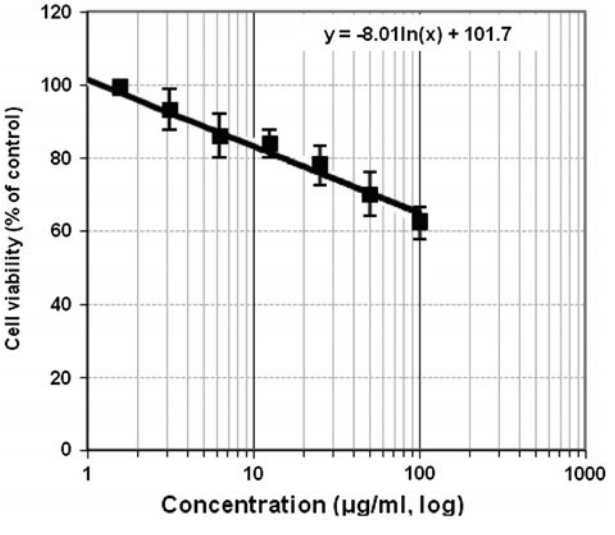

Figure 3. The effect of DMT-1,4-piperazine complex on the proliferation of Hep-G2 cells.

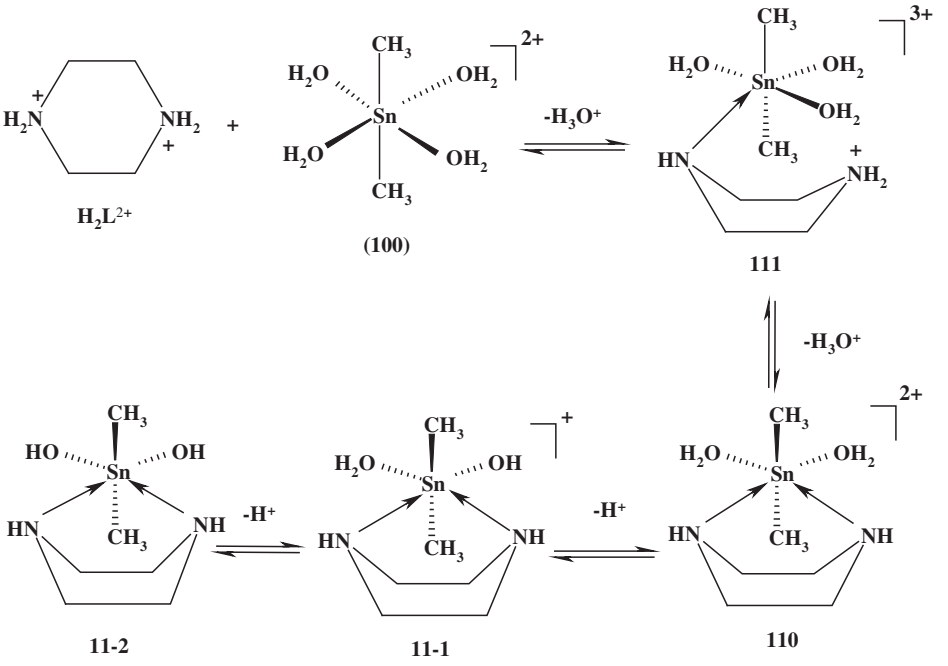

Scheme 1. Formation scheme for dimethyltin(IV)-1,4-piperazine complex.

Table 9. Anti-inflammatory activity of the biologically active compounds.

Compd.	Dose in mg kg^{-1} b.w	Formalin induced rat paw oedema thickness (mm) min^{-1}			
		30	60	90	120
Control	–	8.26 ± 0.066	8.73 ± 0.08	8.5 ± 0.05	7.83 ± 0.061
Dmt.pip	30	7.76 ± 0.045[b]	7.38 ± 0.032[b]	7.19 ± 0.05[b]	6.65 ± 0.044[c]
Indomethacin[a]	60	6.5 ± 0.026[c]	7.19 ± 0.069[b]	7.2 ± 0.071[b]	7.21 ± 0.048[c]

[a]Indomethacin is used as a reference.
[b]Significant at $p < 0.05$.
[c]Significant at $p < 0$.

3.4. *Antitumor activity*

The *in vitro* antitumor activity of the 1,4-piperazine complex shows that the complex exhibits high cell toxicity against Hep-G2 cells as concluded by the high IC50 value, 100 μg mL^{-1}. The effect of the complex on the proliferation of HCT-116 cells revealed that it possessed low cytotoxic effect as indicated by its IC_{50} value, 43.31 μg mL^{-1}. The treatment of 1301 cells with the complex resulted in a non-significant marginal increase in the cell proliferation up to 1.2-fold of the control (lymphoblastic leukemia cells). The results of DMT-1,4-piperazine complex effect on the proliferation of Hep-G2 cells, taken as an example, recorded after 48 h of incubation is displayed in figure 3.

3.5. *Anti-inflammatory activity*

Table 9 shows that dimethyltin(IV) complex of 1,4-piperazine has promising anti-inflammatory activity compared with the reference anti-inflammatory drug, indomethacin.

4. Conclusion

The present study describes the complex formation equilibria of 1,4-piperazine with dimethyltin(IV) ion with formation of 1 : 1 and 1 : 2 complexes. The effect of solvent and temperature on the stability constant of the complexes was investigated. The displacement of 1,4-piperazine coordinated to dimethyltin(IV) by DNA constituents was studied and the results reveal to what extent DNA, the major target in tumor therapy, can displace the coordinated 1,4-piperazine. The 1 : 1 complex was synthesized and characterized. The *in vitro* antitumor activity show that the complex exhibits high cell toxicity against Hep-G2 cells.

Supplemental data

Supplemental data for this article can be accessed here [http://dx.doi.org/10.1080/00958972.2015.1007962].

References

[1] B. Rosenberg. In *Cisplatin: Chemistry and Biochemistry of a Leading Anticancer Drug*, B. Lippert (Ed.), p. 3, Verlag Helvetica Chimica Acta, Zurich; Wiley-VCH, Weinheim (1999).
[2] Y. Yung, S. Lippard. *Chem. Rev.*, **107**, 1387 (2007).
[3] M.A. Jakupec, M. Galanski, V.B. Arion, C.G. Hartinger, B.K. Keppler. *Dalton Trans.*, 183 (2007).
[4] X. Wang, Z. Guo. *Dalton Trans.*, 1521 (2008).
[5] L. Ronconi, P.J. Sadler. *Coord. Chem. Rev.*, **251**, 1633 (2007).
[6] H.K. Adli, N.M. Sidek, N. Ismail, W.M. Khairul. *Empowering Science, Technology and Innovation Toward Better Tomorrow*, 436 (2011).
[7] H.K. Adli, N.M. Sidek, N. Ismail, W.M. Khairul. *Chiang Mai J. Sci.*, **40**, 117 (2013).
[8] (a) S. Khan, S.A.A. Nami, K.S. Siddiqi. *J. Organomet. Chem.*, **693**, 1049 (2008); (b) S. Abbas, S. Ali, M.S. Khan, M. Parvez, J. Iqbal. *J. Coord. Chem.*, **66**, 2765 (2013); (c) J. Anwar, S. Ali, S. Shahzadi, M. Shahid, S.K. Sharma, K. Qanungo. *J. Coord. Chem.*, **66**, 1142 (2013); (d) A. Chilwal, G. Deep, P. Malhotria, A.C. Narula. *J. Coord. Chem.*, **66**, 1046 (2013); (e) T. Sedaghat, L. Tahmasbi, H. Motamedi, R. Reynes-Martinez, D. Morales-Morales. *J. Coord. Chem.*, **66**, 712 (2013); (f) L. Tian, H. Cao, S. Wang, Y. Sun, Z. Liu. *J. Coord. Chem.*, **66**, 624 (2013); (g) Y. Shi, B. Zhang, R. Zhang, S. Zhang. *J. Coord. Chem.*, **65**, 4125 (2012).
[9] Z.A. Siddiqi, M. Shahid, S. Kumar, M. Khalid, S. Noor. *J. Organomet. Chem.*, **694**, 3768 (2009).
[10] M. Nath, H. Singh, G. Eng, X. Song. *Inorg. Chem. Commun.*, **14**, 1381 (2011).
[11] A.Sh. Al-Alousi, M.R. Shehata, M.M. Shoukry, N. Mohamed. *Chem. Spec. Bioavail.*, **21**, 1 (2009).
[12] A. Al-Najjar, M.M.A. Mohamed, M.R. Shehata, M.M. Shoukry. *Annali di Chim.*, **96**, 97 (2006).
[13] A.A. Al-Najjar, M.M.A. Mohamed, M.M. Shoukry. *J. Coord. Chem.*, **59**, 193 (2006).
[14] M.M.A. Mohamed, M.M. Shoukry. *Chem. Pharm. Bull. (Japan)*, **49**, 253 (2001).
[15] O. Al-Flaijj, M.R. Shehata, M.M.A. Mohamed, M.M. Shoukry. *Monatsh. Chem.*, **132**, 349 (2001).
[16] R.G. Bates. *Determination of pH: Theory and Practice*, 2nd edn, Wiley Interscience, New York (1977).
[17] R.J. Motekaitis, A.E. Martell, D.A. Nelson. *Inorg. Chem.*, **23**, 275 (1984).
[18] M.M. Shoukry, M.R. Shehata, M.S.A. Hamza, R. van Eldik. *Dalton Trans.*, 3921 (2005).
[19] P. Gans, A. Sabatini, A. Vacca. *Inorg. Chim. Acta*, **18**, 237 (1976).
[20] L. Pettit. *Personal Communication*, University of Leeds (1993).
[21] M.B. Hansen, S.E. Nielsen, K. Berg. *J. Immunol. Methods*, **119**, 203 (1989).
[22] M. Abdalla Hussein. *Free Rad. Antiox.*, **2**, 44 (2012).
[23] C.A. Winter, E.A. Risley, G.W. Nuss. *Proc. Soc. Exp. Biol. Med.*, **111**, 544 (1962).
[24] D.D. Perrin. *Stability Constants of Metal–Ion Complexes: Part B Organic Ligands*, Pergamon Press, Oxford (1979).

[25] G. Arena, R. Calì, A. Contino, A. Musumeci, S. Musumeci, R. Purrello. *Inorg. Chim. Acta*, **237**, 187 (1995).
[26] T. Natsume, S. Aizawa, K. Hatano, S. Funahashi. *J. Chem. Soc., Dalton Trans.*, 2749 (1994).
[27] N. Buzás, T. Gajda, L. Nagy, E. Kuzmann, A. Vértes, K. Burger. *Inorg. Chim. Acta*, **274**, 167 (1998).
[28] C. De Stefano, C. Foti, A. Gianguzza, M. Martino, L. Pellerito, S. Sammartano. *J. Chem. Eng. Data*, **41**, 511 (1996).
[29] C. Foti, A. Gianguzza, F.J. Millero, S. Sammartano. *Aquat. Geochem.*, **5**, 381 (1999).
[30] T. Soldatović, M. Shoukry, R. Puchta, Z.D. Bugarčić, R. van Eldik. *Eur. J. Inorg. Chem.*, 2261 (2009).
[31] M.R. Shehata, M.M. Shoukry, F.H. Abdel-Shakour, R. van Eldik. *Eur. J. Chem.*, 3912 (2009).
[32] U. Kramer-Schnabel, P.W. Linder. *Inorg. Chem.*, **30**, 1248 (1991).
[33] D.O. Rees. *J. Mol. Biol.*, **141**, 323 (1980).
[34] N.K. Rogers, G.R. Moore, M.J.E. Sternberg. *J. Mol. Biol.*, **182**, 613 (1985).
[35] H. Sigel, R.B. Martin, R. Tribolet, U.K. Haring, R. Malini-Balakrishnan. *Eur. J. Biochem.*, **152**, 187 (1985).
[36] G. Akerlof, O.A. Short. *J. Am. Chem. Soc.*, **75**, 6357 (1953).
[37] M.M. Shoukry, S.M. El-Medani. *Collect. Czech. Chem. Commun.*, **62**, 1023 (1997).
[38] L.C. Mun, M.A. Hapipah, S.K. Shin, A. Sri Nurestri, L.K. Mun. *Appl. Organomet. Chem.*, **26**, 310 (2012).
[39] W. Rehman, M.K. Baloch, A. Badshah, S. Ali. *J. Chin. Chem. Soc.*, **52**, 231 (2005).
[40] M.M. Rahman, I. Jusoh, M. Abu Affan, A. Husaini. *Eur. J. Sci. Res.*, **89**, 512 (2012).
[41] K. Nakamoto. *Infrared and Raman Spectra of Inorganic and Coordination Compounds, Part B: Applications in Coordination Organometallic and Bioinorganic Chemistry*, 6th edn, Wiley, NJ (2009).